J. Mašek, 11.10.2005

New parameterization of cloud optical properties proposed for model ALARO-0

Results of Prague LACE stay 1.8.–1.10.2005
under scientific supervision of Jean-François Geleyn

Main target of this document is to outline design of a new parameterization of cloud optical properties. It does not aim to replace detailed report, which will be prepared later. It is supposed that reader is familiar with the subject, so the basic concepts are not explained here.

1 Introduction

Current radiation scheme used in model ALADIN (in following text referred as old ACRANEB) divides electromagnetic spectrum just in 2 bands – solar and thermal. In each band it applies δ-two stream approximation of radiative transfer equations. With such broad spectral division it is crucial to treat so called saturation effect, caused by wavelength dependency of absorption coefficient k^{abs}, scattering coefficient k^{scat} and asymmetry factor g. What makes this treatment difficult is a non-local dependency of saturation effect on cloud properties (i.e. saturation at given cloud layer depends also on properties and geometry of cloud layers above and below).

However, in old ACRANEB only mean saturation effect is applied locally, regardless of cloud geometry (i.e. the same correction for isolated cloud layer as for vertically developped cloud). Moreover, dependency of liquid/ice cloud optical coefficients $k^{\mathrm{abs}}_{l|i}$, $k^{\mathrm{scat}}_{l|i}$ and $g_{l|i}$ on liquid/ice water content $\rho_{l|i}$ is ignored.

Because radiation scheme is the most expensive physical parameterization in terms of CPU, it was decided to keep 2 spectral bands also in ALARO-0. But since microphysics will provide prognostic cloud water and ice, it is highly desirable to avoid the 2 simplifications of cloud treatment used in old ACRANEB.

2 Strategy of work

New parameterization scheme is based on the same sample of experimental cloud data as the old one. The idea was to create idealized cloud simulation model, which would solve radiative transfer equation in clouds wavelength by wavelength (monochromatic computations), taking into account only diffuse fluxes and ignoring the effect of gases. Spectrally integrated fluxes from these simulations would serve as a reference for parameterized version, they also enable explicit evaluation of saturation effect.

3 Experimental data

Experimental cloud data were kindly provided by Bodo Ritter (DWD). They consist of 3 parts:

1. Data of Stephens for 8 liquid cloud types (cloud liquid water content; volume extinction coefficient, single scattering albedo and asymmetry factor for 107 wavelengths).

2. Data of Röckel et al. for 40 ice cloud types (cloud ice water content; volume extinction coefficient, single scattering albedo and asymmetry factor for 378 wavelengths).

3. Data of Labs and Neckell, resp. Theakara and Drummond for solar insolation at the top of atmosphere (given as weights, i.e. normalized solar energy coming in 102 spectral intervals).

Since the 3 data sources were using different wavelength samplings, it was necessary to preprocess the data. Preprocessing consisted of these steps:

- Selection of 7 liquid clouds[1] and 16 ice clouds with highest ice water content.

- Merging wavelengths from all data sources.

- Dividing wavelengths into spectral bands[2]:

	$\lambda_{\min}$ [μm]	$\lambda_{\max}$ [μm]
solar band	0.300	4.642
thermal band	4.642	105.000

- Conversion of extinction coefficient k^{ext} and single scattering albedo ϖ to absorption and scattering coefficients k^{abs}, k^{scat}.

- Linear interpolation of coefficients k^{abs}, k^{scat} and g into target wavelengths.

- Conversion of volume coefficients [m^{-1}] into mass coefficients[3] [$\text{m}^2 \cdot \text{kg}^{-1}$]:

$$(k_{l|i})_{\text{mass}} = \frac{(k_{l|i})_{\text{vol}}}{\rho_{l|i}}$$

- Conversion of solar weights into weight function (spectral energy density), interpolation to target wavelengths assuming stepwise dependency.

- Computation of thermal weight function (Planck function $B_\lambda(T)$ with temperature $T = 255.8\,\text{K}$) for target wavelengths.

[1] Type stratocumulus 2 was excluded, since it was spoiling the fits.

[2] Solar band in ALADIN is wider, covering part of UV region where intense O_3 absorption takes place. Liquid cloud data were restricted by $\lambda = 0.300\,\mu$m. This can be afforded in cloud model, where gaseous absorption is ignored. Less than 1% of solar insolation belongs to neglected UV region.

[3] In ALADIN mass coefficients are further divided by gravity acceleration, which gives units [Pa^{-1}].

4 Cloud simulation model 0

Cloud simulation model 0 performs monochromatic computations for homogeneous cloud (only one cloud layer with liquid water content ρ_l, ice water content ρ_i, geometrical depth Δz and cloud fraction $n = 1$). In each spectral band it is assumed that cloud is illuminated from the top by diffuse radiation with spectral composition given by weight function w_λ. In this case outgoing monochromatic fluxes at layer bottom and top are given by:

$$\begin{bmatrix} F^{\downarrow}_{B\lambda} \\ F^{\uparrow}_{T\lambda} \end{bmatrix} = \begin{bmatrix} a_{4\lambda} & a_{5\lambda} \\ a_{5\lambda} & a_{4\lambda} \end{bmatrix} \cdot \begin{bmatrix} w_\lambda \\ 0 \end{bmatrix} \tag{1}$$

Monochromatic layer transmittance $a_{4\lambda}$ and reflectance $a_{5\lambda}$ can be expressed via quantities k^{abs}_λ, $k^{\mathrm{scat}}_\lambda$, g_λ, ρ_l, ρ_i and Δz. But before, first three of these quantities must be obtained by following procedure (steps denoted by primes are for later use):

A1) Fitting of $k^{\mathrm{abs}}_{l\lambda}$, $k^{\mathrm{scat}}_{l\lambda}$, $g_{l\lambda}$ to ρ_l:

$$\begin{aligned} \ln k^{\mathrm{abs}}_{l\lambda} &= a^{\mathrm{abs}}_{l\lambda} \sqrt{\rho_l} + b^{\mathrm{abs}}_{l\lambda} \\ \ln k^{\mathrm{scat}}_{l\lambda} &= a^{\mathrm{scat}}_{l\lambda} \sqrt{\rho_l} + b^{\mathrm{scat}}_{l\lambda} \\ \ln g_{l\lambda} &= a_{l\lambda} \ln \rho_l + b_{l\lambda} \end{aligned} \tag{2}$$

Values of $g_{l\lambda}$ greather than 1 are truncated to 1.

A2) Fitting of $k^{\mathrm{abs}}_{i\lambda}$, $k^{\mathrm{scat}}_{i\lambda}$, $g_{i\lambda}$ to ρ_i:

$$\begin{aligned} \ln k^{\mathrm{abs}}_{i\lambda} &= a^{\mathrm{abs}}_{i\lambda} \ln \rho_i + b^{\mathrm{abs}}_{i\lambda} \\ \ln k^{\mathrm{scat}}_{i\lambda} &= a^{\mathrm{scat}}_{i\lambda} \ln \rho_i + b^{\mathrm{scat}}_{i\lambda} \\ \ln g_{i\lambda} &= a_{i\lambda} \ln \rho_i + b_{i\lambda} \end{aligned} \tag{3}$$

Here it must be checked that $a^{\mathrm{abs}}_{i\lambda}, a^{\mathrm{scat}}_{i\lambda} \geq -1$. It is necessary for having finite optical depth in $\rho_i \to 0$ limit. Again, values of $g_{i\lambda}$ greather than 1 are truncated to 1.

A2') Spectral averaging[4] of asymmetry factors $g_{l\lambda}$, $g_{i\lambda}$:

$$g_l = \frac{\int_{\Delta\lambda} g_{l\lambda} k^{\mathrm{scat}}_\lambda w_\lambda \,\mathrm{d}\lambda}{\int_{\Delta\lambda} k^{\mathrm{scat}}_\lambda w_\lambda \,\mathrm{d}\lambda} \qquad g_i = \frac{\int_{\Delta\lambda} g_{i\lambda} k^{\mathrm{scat}}_\lambda w_\lambda \,\mathrm{d}\lambda}{\int_{\Delta\lambda} k^{\mathrm{scat}}_\lambda w_\lambda \,\mathrm{d}\lambda} \tag{4}$$

A3) δ-scaling of $k^{\mathrm{abs}}_{l\lambda}$, $k^{\mathrm{abs}}_{i\lambda}$, $k^{\mathrm{scat}}_{l\lambda}$, $k^{\mathrm{scat}}_{i\lambda}$:

$$\begin{aligned} k^{\mathrm{abs}}_{l\lambda} &\mapsto k^{\mathrm{abs}}_{l\lambda} \\ k^{\mathrm{abs}}_{i\lambda} &\mapsto k^{\mathrm{abs}}_{i\lambda} \\ k^{\mathrm{scat}}_{l\lambda} &\mapsto k^{\mathrm{scat}}_{l\lambda} \cdot (1 - {g_{l\lambda}}^2) \\ k^{\mathrm{scat}}_{i\lambda} &\mapsto k^{\mathrm{scat}}_{i\lambda} \cdot (1 - {g_{i\lambda}}^2) \end{aligned} \tag{5}$$

[4] All integrals were evaluated using trapezoidal rule.

A3') Spectral averaging of δ-scaled $k_{l\lambda}^{\mathrm{abs}}$, $k_{i\lambda}^{\mathrm{abs}}$, $k_{l\lambda}^{\mathrm{scat}}$, $k_{i\lambda}^{\mathrm{scat}}$ (subscript 0 denotes unsaturated values):

$$\begin{aligned} k_{0l}^{\mathrm{abs}} &= \frac{\int_{\Delta\lambda} k_{l\lambda}^{\mathrm{abs}} w_\lambda \,\mathrm{d}\lambda}{\int_{\Delta\lambda} w_\lambda \,\mathrm{d}\lambda} \qquad & k_{0i}^{\mathrm{abs}} &= \frac{\int_{\Delta\lambda} k_{i\lambda}^{\mathrm{abs}} w_\lambda \,\mathrm{d}\lambda}{\int_{\Delta\lambda} w_\lambda \,\mathrm{d}\lambda} \\ k_{0l}^{\mathrm{scat}} &= \frac{\int_{\Delta\lambda} k_{l\lambda}^{\mathrm{scat}} w_\lambda \,\mathrm{d}\lambda}{\int_{\Delta\lambda} w_\lambda \,\mathrm{d}\lambda} \qquad & k_{0i}^{\mathrm{scat}} &= \frac{\int_{\Delta\lambda} k_{i\lambda}^{\mathrm{scat}} w_\lambda \,\mathrm{d}\lambda}{\int_{\Delta\lambda} w_\lambda \,\mathrm{d}\lambda} \end{aligned} \tag{6}$$

A4) Merging of liquid and ice quantities:

$$k_\lambda^{\mathrm{abs}} = \frac{\rho_l k_{l\lambda}^{\mathrm{abs}} + \rho_i k_{i\lambda}^{\mathrm{abs}}}{\rho_l + \rho_i} \qquad k_\lambda^{\mathrm{scat}} = \frac{\rho_l k_{l\lambda}^{\mathrm{scat}} + \rho_i k_{i\lambda}^{\mathrm{scat}}}{\rho_l + \rho_i} \qquad g_\lambda = \frac{\rho_l g_{l\lambda} + \rho_i g_{i\lambda}}{\rho_l + \rho_i} \tag{7}$$

A4') Merging of broadband liquid and ice quantities:

$$k_0^{\mathrm{abs}} = \frac{\rho_l k_{0l}^{\mathrm{abs}} + \rho_i k_{0i}^{\mathrm{abs}}}{\rho_l + \rho_i} \qquad k_0^{\mathrm{scat}} = \frac{\rho_l k_{0l}^{\mathrm{scat}} + \rho_i k_{0i}^{\mathrm{scat}}}{\rho_l + \rho_i} \qquad g = \frac{\rho_l g_l + \rho_i g_i}{\rho_l + \rho_i} \tag{8}$$

Finally, monochromatic coefficients a_4, a_5 can be evaluated (index λ was omitted for brevity):

$$a_4 = \frac{\tau(1-\rho^2)}{(1-\tau^2\rho^2)} \qquad a_5 = \frac{\rho(1-\tau^2)}{(1-\tau^2\rho^2)} \tag{9}$$

$$\begin{aligned} &\tau \equiv \exp[-\epsilon(k^{\mathrm{abs}} + k^{\mathrm{scat}})(\rho_l + \rho_i)\Delta z] \qquad && \alpha_1 \equiv 2[1 - \varpi(1-\beta)] \qquad && \beta \equiv \frac{4+g}{8(1+g)} \\ &\rho \equiv \frac{\alpha_2}{\alpha_1 + \epsilon} && \alpha_2 \equiv 2\varpi\beta && \varpi \equiv \frac{k^{\mathrm{scat}}}{k^{\mathrm{abs}} + k^{\mathrm{scat}}} \\ &\epsilon \equiv \sqrt{\alpha_1^2 - \alpha_2^2} \end{aligned}$$

Variables (τ, ρ) in relations (9) are dimensionless auxiliary quantities, i.e. ρ has nothing to do with density.

Having monochromatic coefficients $a_{4\lambda}$, $a_{5\lambda}$, monochromatic outgoing fluxes $F_{B\lambda}^{\downarrow}$, $F_{T\lambda}^{\uparrow}$ can be evaluated using relation (1). Then they can be spectrally integrated to get broadband fluxes $F_B^{\downarrow}$, $F_T^{\uparrow}$ and normalized by broadband incoming flux, which gives broadband cloud transmittance a_4 and reflectance a_5:

$$a_4 = \frac{\int_{\Delta\lambda} a_{4\lambda} w_\lambda \,\mathrm{d}\lambda}{\int_{\Delta\lambda} w_\lambda \,\mathrm{d}\lambda} \qquad a_5 = \frac{\int_{\Delta\lambda} a_{5\lambda} w_\lambda \,\mathrm{d}\lambda}{\int_{\Delta\lambda} w_\lambda \,\mathrm{d}\lambda} \tag{10}$$

Broadband coefficients a_4, a_5 can be inverted to saturated coefficients k^{abs}, k^{scat} using relations (9). Inversion proceeds as follows:

- Inversion of a_4, a_5 to τ, ρ.
- Computation of broadband back scatter fraction β from broadband asymmetry factor g (result of step A4').
- Inverting ρ to ϖ (this is possible since β is known).
- Computation of α_1, α_2 from ϖ, β.
- Inversion of τ to $k^{\mathrm{ext}} \equiv k^{\mathrm{abs}} + k^{\mathrm{scat}}$.
- Splitting k^{ext} to k^{abs}, k^{scat} using ϖ.

Resulting broadband coefficients k^{abs}, k^{scat} represent saturated values. They can be compared with unsaturated values k_0^{abs}, k_0^{scat} (i.e. saturated values in $\Delta z \to 0$ limit) obtained by step A4'.

Outputs from cloud simulation model 0 are broadband cloud transmittance a_4 and reflectance a_5, as well as saturation factors c^{abs}, c^{scat} defined by formulas:

$$c^{\mathrm{abs}} \equiv \frac{k^{\mathrm{abs}}}{k_0^{\mathrm{abs}}} \qquad c^{\mathrm{scat}} \equiv \frac{k^{\mathrm{scat}}}{k_0^{\mathrm{scat}}} \tag{11}$$

Central result of the work was finding that dependency of saturation factors c^{abs}, c^{scat} versus unsaturated optical depth $\delta_0 \equiv (k_0^{\mathrm{abs}} + k_0^{\mathrm{scat}})(\rho_l + \rho_i)\Delta z$ is very sharp in solar band, regardless of liquid/ice water content, geometrical depth or cloud inhomogenity. It can be fitted with simple function of the type:

$$c = \frac{1}{1 + \left(\dfrac{\delta_0}{\delta_0^{\mathrm{crit}}}\right)^{\mu}} \tag{12}$$

Here δ_0^{crit} denotes value of δ_0 for which $c = 0.5$ and μ is sharpness parameter. Requirements that $c \to 1$ as $\delta_0 \to 0$ and that saturated optical depth δ increases monotonically with δ_0 restrict range of permissible μ values to $0 < \mu \leq 1$.

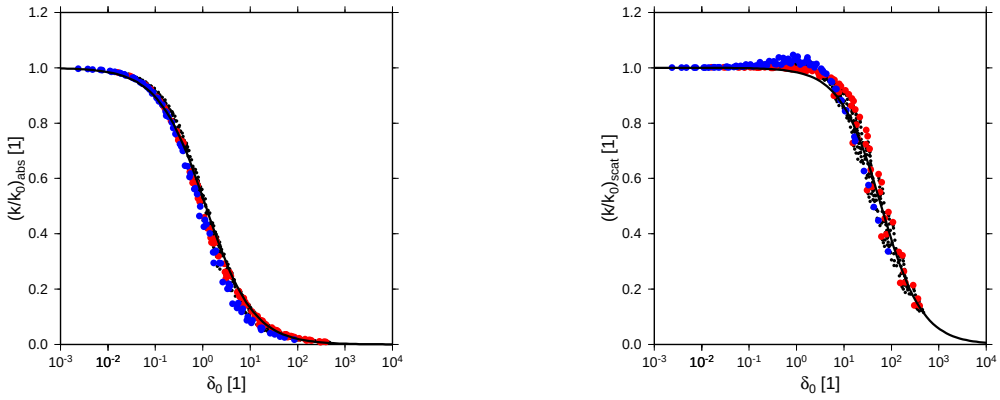

Figure 1: Dependency of saturation factors c^{abs} (left) and c^{scat} (right) on unsaturated optical depth δ_0 in solar band. Sample of homogeneous clouds. Red dots – liquid clouds, blue dots – ice clouds, black dots – mixed clouds, black lines – fitted dependencies.

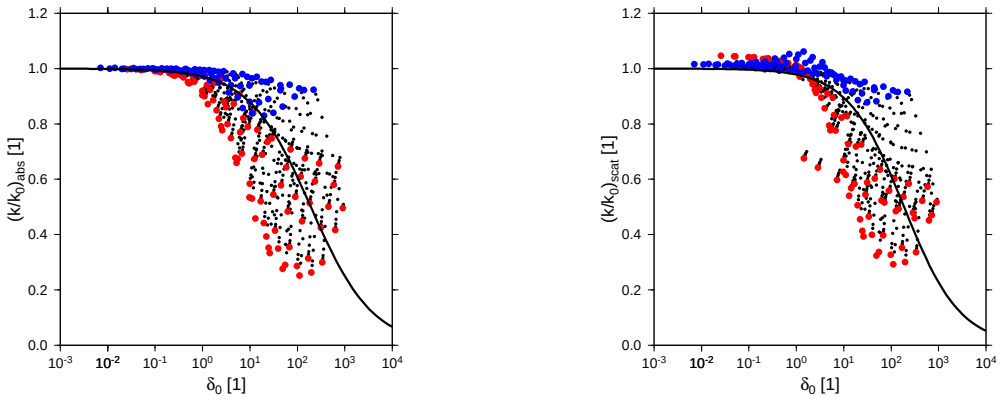

Figure 2: Dependency of saturation factors c^{abs} (left) and c^{scat} (right) on unsaturated optical depth δ_0 in thermal band. Sample of homogeneous clouds. Red dots – liquid clouds, blue dots – ice clouds, black dots – mixed clouds, black lines – fitted dependencies.

In thermal band dependency of c^{abs}, c^{scat} on δ_0 loses its sharpness for $\delta_0 \gtrsim 1$. But this does not pose a serious problem since in this case fluxes are already close to blackbody radiation.

Remarks:

1. Scalings for fits (2), (3) were found by trial and error. In order to have robust fitting procedure, it was decided to use linear relations between scaled monochromatic quantities and scaled liquid/ice water content. Optimal scalings were judged by looking at dependency of scaled *broadband* quantities, which should be as close to linear as possible.

2. For some wavelengths single scattering albedo ϖ can be 1, which means $k^{\mathrm{abs}} = 0$. To treat such cases $\ln(k^{\mathrm{abs}})$ in fits (2), (3) was replaced by $\ln[\max(k^{\mathrm{abs}}, \varepsilon)]$ with $\varepsilon = 10^{-5}$.

3. Inversion from a_4, a_5 to τ, ρ can cause numerical problems for $a_4 \approx 0$ (this happens for thick clouds in thermal band). In such cases inverse formulas for τ and ρ were approximated by their truncated power series in a_4. Cases $a_4 = 0$ (with machine precision) were ignored, since they would lead to infinite value of extinction coefficient k^{ext}, which is unphysical.

4. In model ALARO-0 broadband coefficients k_{0l}^{abs}, k_{0i}^{abs}, k_{0l}^{scat}, k_{0i}^{scat} (resp. g_l, g_i) will not be determined via steps A1–A3, A3' (resp. A1, A2, A2'). This would be too costly, moreover it would require having monochromatic cloud data in the model. Instead, results of these procedures will be fitted directly to ρ_l, ρ_i for wide range of their values, using Pade approximants with suitable scalings. So far only preliminary Pade approximants were found. They are not fully satisfactory for thermal scattering case, as can be seen from the right plot on figure 2 (there is a separation between liquid and ice clouds for $\delta_0 \ll 1$ and saturation factor c^{scat} does not tend exactly to 1 as $\delta_0 \to 0$ neither for liquid, nor for ice clouds).

5 Cloud simulation model 1

Cloud simulation model 1 performs monochromatic computations for non-homogeneous multi-layer cloud, taking into account cloud geometry. Individual cloud layers are assumed homogeneous, with liquid water content ρ_{lj}, ice water content ρ_{ij}, geometrical thickness Δz_j and cloud fraction n_j. Optical properties of each layer are computed in the same way as for homogeneous cloud. Overlaps between adjacent cloud layers can be either random or maximum[5]. Again, it is assumed that in each spectral band cloud is illuminated from the top by diffuse radiation with spectral composition given by weight function w_λ.

For each layer $j = 1, \ldots, J$ (numbering starts from the top) there are 2 systems relating incoming and outgoing fluxes. One for cloud free part F, the other for cloudy part C:

$$\begin{aligned}
\begin{bmatrix} F^{\downarrow F}_{B\lambda} \\ F^{\uparrow F}_{T\lambda} \end{bmatrix}_j &= \begin{bmatrix} 1 & 0 \\ 0 & 1 \end{bmatrix} \cdot \begin{bmatrix} F^{\downarrow F}_{T\lambda} \\ F^{\uparrow F}_{B\lambda} \end{bmatrix}_j \\
\begin{bmatrix} F^{\downarrow C}_{B\lambda} \\ F^{\uparrow C}_{T\lambda} \end{bmatrix}_j &= \begin{bmatrix} a_{4\lambda} & a_{5\lambda} \\ a_{5\lambda} & a_{4\lambda} \end{bmatrix}_j \cdot \begin{bmatrix} F^{\downarrow C}_{T\lambda} \\ F^{\uparrow C}_{B\lambda} \end{bmatrix}_j
\end{aligned} \tag{13}$$

At layer interfaces, fluxes leaving one layer must be redistributed between cloudy and cloud free parts of the next layer:

$$\begin{aligned}
\begin{bmatrix} F^{\downarrow F}_{T\lambda} \\ F^{\downarrow C}_{T\lambda} \end{bmatrix}_j &= \begin{bmatrix} b_1 & 1-b_3 \\ 1-b_1 & b_3 \end{bmatrix}_j \cdot \begin{bmatrix} F^{\downarrow F}_{B\lambda} \\ F^{\downarrow C}_{B\lambda} \end{bmatrix}_{j-1} \\
\begin{bmatrix} F^{\uparrow F}_{B\lambda} \\ F^{\uparrow C}_{B\lambda} \end{bmatrix}_j &= \begin{bmatrix} b_2 & 1-b_4 \\ 1-b_2 & b_4 \end{bmatrix}_j \cdot \begin{bmatrix} F^{\uparrow F}_{T\lambda} \\ F^{\uparrow C}_{T\lambda} \end{bmatrix}_{j+1}
\end{aligned} \tag{14}$$

Redistribution weights b_{1j}, b_{2j}, b_{3j}, b_{4j} depend on cloud overlapping mode. They can be expressed as:

	random overlaps	maximum overlaps
b_{1j}	$1 - n_j$	$\frac{1-\max(n_j,n_{j-1})}{1-n_{j-1}}$ (1 for $n_{j-1} = 1$)
b_{2j}	$1 - n_j$	$\frac{1-\max(n_j,n_{j+1})}{1-n_{j+1}}$ (1 for $n_{j+1} = 1$)
b_{3j}	n_j	$\frac{\min(n_j,n_{j-1})}{n_{j-1}}$ (1 for $n_{j-1} = 0$)
b_{4j}	n_j	$\frac{\min(n_j,n_{j+1})}{n_{j+1}}$ (1 for $n_{j+1} = 0$)

System (13), (14) is completed with boundary conditions:

$$\begin{aligned}
(F^{\downarrow F}_{T\lambda})_1 &= (1-n_1)w_\lambda & (F^{\downarrow C}_{T\lambda})_1 &= n_1 w_\lambda \\
(F^{\uparrow F}_{B\lambda})_J &= 0 & (F^{\uparrow C}_{B\lambda})_J &= 0
\end{aligned} \tag{15}$$

[5]More distant cloud layers are independent to the extent allowed by requirement of maximum overlaps between adjacent layers.

By elimination of incoming fluxes between layers, equations (13), (14), (15) can be compacted into 3-diagonal system with blocks consisting of 4×4 matrices (subscript λ was omitted for brevity):

$$\begin{bmatrix} B_1 & C_1 & & & & \\ A_2 & B_2 & C_2 & & & \\ & A_3 & B_3 & C_3 & & \\ & & \ddots & \ddots & \ddots & \\ & & & A_{J-1} & B_{J-1} & C_{J-1} \\ & & & & A_J & B_J \end{bmatrix} \cdot \begin{bmatrix} F_1 \\ F_2 \\ F_3 \\ \vdots \\ F_{J-1} \\ F_J \end{bmatrix} = \begin{bmatrix} S_1 \\ S_2 \\ S_3 \\ \vdots \\ S_{J-1} \\ S_J \end{bmatrix} \tag{16}$$

$$A_j = \begin{bmatrix} -b_{1j} & 0 & -(1-b_{3j}) & 0 \\ 0 & 0 & 0 & 0 \\ -a_{4j}(1-b_{1j}) & 0 & -a_{4j}b_{3j} & 0 \\ -a_{5j}(1-b_{1j}) & 0 & -a_{5j}b_{3j} & 0 \end{bmatrix} \qquad B_j = \begin{bmatrix} 1 & 0 & 0 & 0 \\ 0 & 1 & 0 & 0 \\ 0 & 0 & 1 & 0 \\ 0 & 0 & 0 & 1 \end{bmatrix} \qquad S_1 = \begin{bmatrix} (1-n_1)w \\ 0 \\ a_{41}n_1 w \\ a_{51}n_1 w \end{bmatrix}$$

$$C_j = \begin{bmatrix} 0 & 0 & 0 & 0 \\ 0 & -b_{2j} & 0 & -(1-b_{4j}) \\ 0 & -a_{5j}(1-b_{2j}) & 0 & -a_{5j}b_{4j} \\ 0 & -a_{4j}(1-b_{2j}) & 0 & -a_{4j}b_{4j} \end{bmatrix} \qquad F_j = \begin{bmatrix} F_{Bj}^{\downarrow F} \\ F_{Tj}^{\uparrow F} \\ F_{Bj}^{\downarrow C} \\ F_{Tj}^{\uparrow C} \end{bmatrix} \qquad S_2 = \cdots = S_J = 0$$

System (16) can be solved by elimination and back-substitution:

$$\begin{aligned} \tilde{B}_1 &= B_1 & \tilde{S}_1 &= S_1 \\ \tilde{B}_j &= B_j - A_j \tilde{B}_{j-1}^{-1} C_{j-1} & \tilde{S}_j &= S_j - A_j \tilde{B}_{j-1}^{-1} \tilde{S}_{j-1} \qquad j = 2, \ldots, J \end{aligned}$$

$$\begin{aligned} F_J &= \tilde{B}_J^{-1} \tilde{S}_J \\ F_j &= \tilde{B}_j^{-1} (\tilde{S}_j - C_j F_{j+1}) \qquad j = J-1, \ldots, 1 \end{aligned} \tag{17}$$

Results from cloud simulation model 1 are outgoing monochromatic fluxes for cloud free part F and cloudy part C of each layer. At cloud bottom and top they are summed together (F + C) and spectrally integrated, in order to get total broadband outgoing fluxes. These are normalized by total broadband incoming flux, giving broadband cloud transmittance a_4 and reflectance a_5.

Remark:

For multi-layer cloud with geometry it is possible to define *global* saturation factors c^{abs}, c^{scat} by requirement that cloud with broadband optical coefficients

$$\begin{aligned} k_j^{\mathrm{abs}} &= c^{\mathrm{abs}} k_{0j}^{\mathrm{abs}} \\ k_j^{\mathrm{scat}} &= c^{\mathrm{scat}} k_{0j}^{\mathrm{scat}} \end{aligned} \qquad j = 1, ..., J$$

gives the same total broadband outgoing fluxes as the reference cloud computed monochromatically. Unlike homogeneous case, inversion from cloud a_4, a_5 to c^{abs}, c^{scat} must be done numerically, which makes this procedure very costly.

6 Outline of the new parameterization

New parameterization of cloud optical properties is based on fits (12) obtained for homogeneous cloud sample. Remaining problem is how to generalize unsaturated optical depth δ_0 to multi-layer case with geometry. It was decided not to apply saturation correction globally for whole cloud, but separately for each cloud layer. This can be achieved by above–central–below decomposition based on two steps:

B1) For each cloud layer, cloud layers above/below are transformed into equivalent homogeneous "rectangular" cloud. Transformation is based on purely geometrical considerations, conserving the total mass of liquid/ice water and moist air *inside* the cloud. It is therefore common for both spectral bands. Result is a 3-layer cloud composed of these homogeneous layers:

cloud above ... (a)
central layer ... (c)
cloud below ... (b)

Conservation of total liquid/ice water mass leads to the relation for liquid/ice water path in equivalent cloud:

$$\rho_{l|i}\Delta z = \frac{1}{a_g \overline{n}} \sum_k n_k (q_{l|i})_k \Delta p_k \qquad \begin{array}{l} \text{cloud above: } k = j_{\min}, \ldots, j-1 \\ \text{cloud below: } k = j+1, \ldots, j_{\max} \end{array} \tag{18}$$

Index j denotes central layer, $j_{\min}$ and $j_{\max}$ are the first and the last layer with non-zero cloud fraction, a_g is gravity acceleration, $\overline{n}$ is mean cloudiness for the cloud above/below, $(q_{l|i})_k$ is specific mass of liquid/ice water for layer k and Δp_k is pressure difference across the layer.

In order to include effect of cloud geometry, mean cloudiness $\overline{n}$ is not computed as simple arithmetic average of n_k (this would give the same result for maximum and random overlaps), but rather as:

$$\overline{n} = \frac{\sum_k n_{k-1,k}}{\sum_k 1} \qquad \begin{array}{l} \text{cloud above: } k = j_{\min}+1, \ldots, j-1 \\ \text{cloud below: } k = j+2, \ldots, j_{\max} \end{array} \tag{19}$$

Quantity $n_{k-1,k}$ denotes total cloudiness for layers $k-1$ and k, so it depends on cloud overlapping mode. If the cloud above/below is composed of isolated parts separated by two or more cloud free layers, its mean cloudiness $\overline{n}$ will be reduced. This mechanism should at least partially simulate effect of gases, due to which there is weaker saturation when the cloud layers are separated.

The last step needed to get liquid/ice water content of equivalent cloud above/ below is to determine its geometrical depth Δz. It can be obtained from conservation of moist air mass inside the cloud. Assumption that equivalent cloud has the same moist air density as central layer j gives:

$$\Delta z = \frac{R_j T_j}{p_j} \frac{1}{a_g \overline{n}} \sum_k n_k \Delta p_k \qquad \begin{array}{l} \text{cloud above: } k = j_{\min}, \ldots, j-1 \\ \text{cloud below: } k = j+1, \ldots, j_{\max} \end{array} \tag{20}$$

Quantity R_j is gas constant of moist air for central layer j, T_j is temperature and p_j is pressure.

B2) For resulting 3-layer cloud effective δ_0 is computed as:

$$\delta_0^{\text{eff}} \equiv \frac{n_a\delta_{0a} + n_c\delta_{0c} + n_b\delta_{0b}}{n} \tag{21}$$

Here n is total cloudiness of the 3-layer cloud, depending on cloud fractions n_a, n_c, n_b and cloud overlapping mode:

$$\begin{aligned} &\text{random overlaps:} && 1-n = (1-n_a)(1-n_c)(1-n_b) \\ &\text{maximum overlaps:} && 1-n = \frac{[1-\max(n_a,n_c)][1-\max(n_c,n_b)]}{1-n_c} \end{aligned}$$

In case of trivial geometry $n_a = n_c = n_b = n$ (for random overlaps it means $n = 1$), formula (21) reduces to sum of optical depths, which is required behaviour. On the other hand, since $n_{\text{rand}} \geq n_{\max}$, optical depth δ_0^{eff} will be smaller for random overlaps, leading to weaker saturation. This is also desired behaviour, since mean geometrical thickness of the cloud is smaller for random overlaps.

Proposed new parameterization of cloud optical properties can be summarized now:

- loop through layers
  - determine $\rho_{l|i}$, Δz and $\overline{n}$ for equivalent cloud above/below
  - loop through spectral bands
    - loop through a–c–b
      - determine broadband optical coefficients k_{0l}^{abs}, k_{0i}^{abs}, k_{0l}^{scat}, k_{0i}^{scat}, g_l and g_i using Pade approximants
      - merge liquid and ice quantities to k_0^{abs}, k_0^{scat} and g using formulas (8)
      - compute unsaturated optical depth δ_0
    - end of loop through a–c–b
    - compute total cloudiness n for 3-layer cloud a–c–b
    - compute δ_0^{eff} using formula (21)
    - determine saturation factors c^{abs}, c^{scat} using fits (12)
    - for central layer compute saturated coefficients k^{abs}, k^{scat} and convert g to β
  - end of loop through spectral bands
- end of loop through layers

7 Preliminary results

So far, new parameterization scheme was tested only for sample of homogeneous clouds and for limited samples of 3-layer non-homogeneous clouds and 3-layer clouds with geometry (i.e. step B1 was not needed). Cloud simulation models 0 and 1 were used as reference. Evaluation of the new scheme was based on scatterplots of parameterized versus reference broadband cloud transmittance a_4 and reflectance a_5. New scheme gives encouraging results compared to the old one (see figures 3–6), but it must be remembered that they were obtained in idealized framework neglecting effect of gases. Because of this, performance in full model will be somewhat deteriorated.

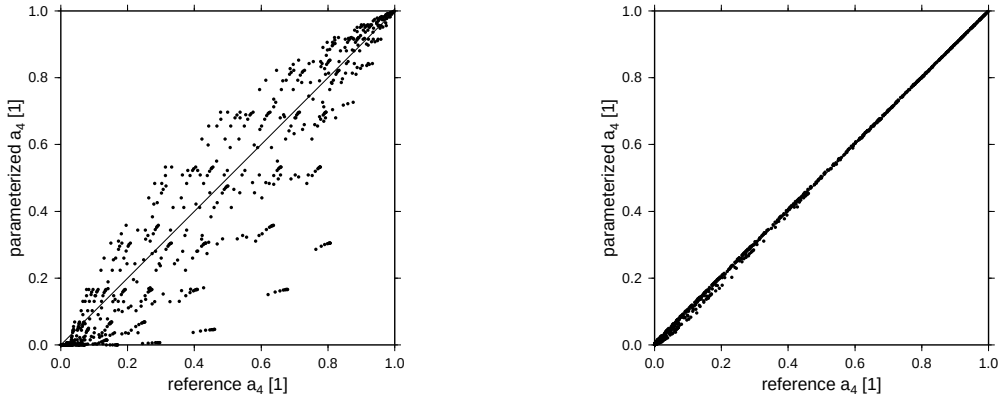

Figure 3: Parameterized versus reference cloud transmittance a_4 for old scheme (left) and new scheme (right). Sample of homogeneous clouds, solar band.

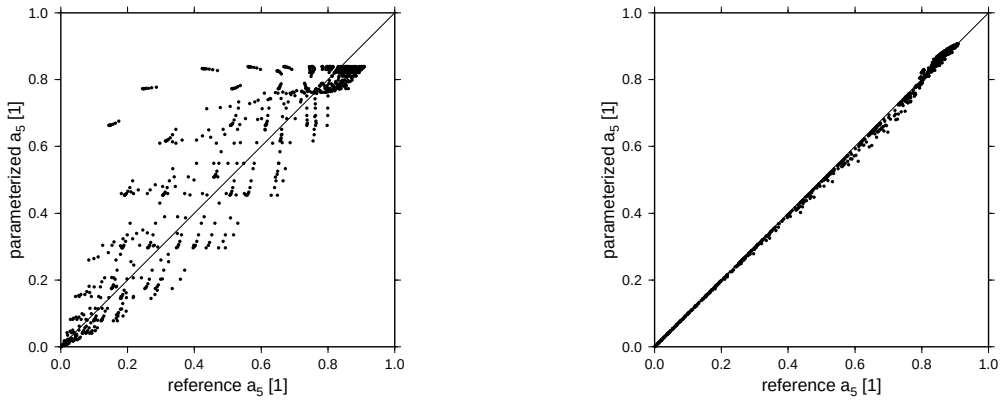

Figure 4: Parameterized versus reference cloud reflectance a_5 for old scheme (left) and new scheme (right). Sample of homogeneous clouds, solar band.

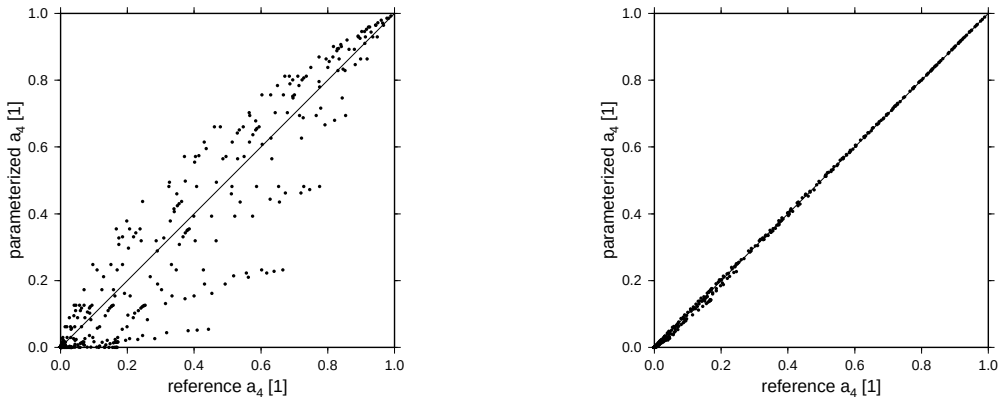

Figure 5: Parameterized versus reference cloud transmittance a_4 for old scheme (left) and new scheme (right). Sample of homogeneous clouds, thermal band.

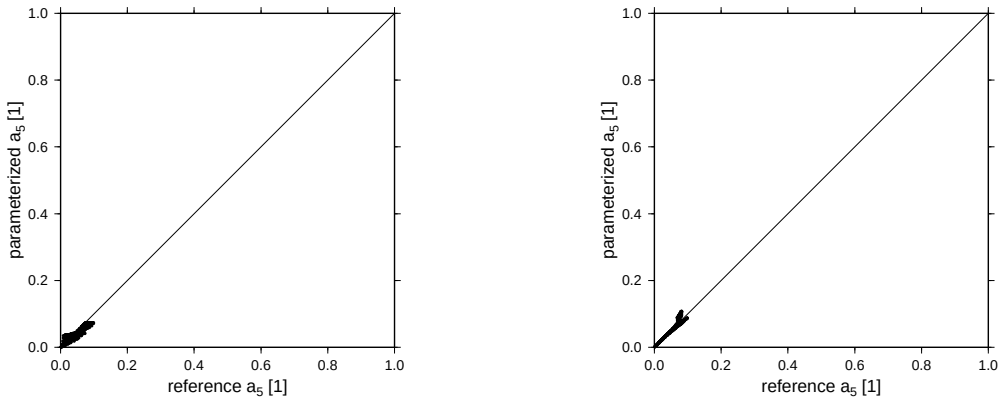

Figure 6: Parameterized versus reference cloud reflectance a_5 for old scheme (left) and new scheme (right). Sample of homogeneous clouds, thermal band.

8 Remaining work

1. Implementation of complete parameterization scheme (including the step B1) and testing it for $J > 3$.

2. Coding final form of parameterization scheme for ALARO-0.

3. Improving the Pade approximants for k_{0l}^{abs}, k_{0i}^{abs}, k_{0l}^{scat}, k_{0i}^{scat}, g_l and g_i, especially for scattering coefficients in thermal band.

4. Writing a detailed report.